

Multi-bandgap photonic materials and devices fabricated by UV-laser induced quantum well intermixing*

Mohammad Kaleem**, ZHANG Xin (张欣), YANG You-guang (杨友光), ZHUANG Yuan (庄园), and HE Jian-jun (何建军)

State Key Laboratory of Modern Optical Instrumentation, Department of Optical Engineering, Zhejiang University, Hangzhou 310027, China

(Received 11 May 2013)

©Tianjin University of Technology and Springer-Verlag Berlin Heidelberg 2013

Ultraviolet (UV)-laser induced quantum well intermixing (QWI) technique can generate large multiple bandgap blue shifts in III-V quantum well semiconductor heterostructure. The application of the UV-laser QWI technique to fabricate multi-bandgap photonic devices based on compressively strained InGaAsP/InP quantum well laser microstructure is reported. We show that under certain UV-laser irradiation conditions, the photoluminescence (PL) intensity can be enhanced, and the full width at half maximum (FWHM) linewidth can be reduced. The blue shift of bandgap can reach as large as 145 nm, while the PL intensity is about 51% higher than that of the as-grown material. Experimental results of post growth wafer level processing for the fabrication of bandgap-shifted waveguides and laser diodes are presented.

Document code: A **Article ID:** 1673-1905(2013)05-0358-4

DOI 10.1007/s11801-013-3088-1

Many quantum well intermixing (QWI) techniques have been developed, including impurity-induced disordering (IID), impurity-free vacancy disordering (IFVD)^[1,2], ion implantation induced disordering (IIID)^[3,4], argon plasma induced disordering^[5] and plasma induced damage during the deposition of sputtered SiO₂^[6,7]. UV-laser induced disordering QWI technique is one of the promising techniques reported in Refs.[7-11]. The technique consists of two steps. Firstly, UV-laser irradiation creates point defects near the surface of quantum well (QW) material. Secondly, rapid thermal annealing (RTA) process is used to diffuse these point defects downwards the QW region, which leads to large bandgap energy shift. InP sacrificial layer is commonly used as a pool of point defects generated by UV-laser. The exchange of group V elements, e.g. P and As, and group III elements, e.g. Ga and In, can cause alteration of the well width and the potential barrier height. This leads to the blue shifts of the optical absorption edge and the creation of a multiple bandgaps QW material. It enables the post growth wafer level fabrication of multi-bandgap QW material, which facilitates active and passive components to be integrated monolithically at relatively reduced cost.

Absorption of UV-laser radiation by solids is known to induce disorder to the lattice and lead to the intermixing effect. Furthermore, the bond strength of InP is weaker

than that of InGaAs^[8]. Thus, we can achieve higher concentration of point defects with even lower UV-laser fluence in InP top sacrificial layer while the InGaAs surface remains undamaged. It is necessary for the fabrication of photonic devices on the QWI altered material. Therefore, the altered material can have high optical and electrical quality.

Previous blue shift of 107–130 nm using unstrained InGaAs/InGaAsP quantum well laser structure has been reported^[8-10]. In this paper, some superior experimental results with wavelength blue-shifts of 145 nm in compressively strained InGaAsP/InP QW laser structure using the combination of UV-laser irradiation and rapid thermal annealing process are presented. We show that the photoluminescence (PL) intensity can be enhanced with reduced full width at half maximum (FWHM) linewidth under certain UV-laser irradiation conditions. A thick InP sacrificial layer, which is removed after UV-laser irradiation and RTA, also ensures little surface damage which may affect the device performance. We present the preliminary results on the application of the UV-laser QWI technique for multi-bandgap waveguide and FP-laser fabrication.

The investigated sample of InGaAsP/InP laser structure was grown using standard metal-organic chemical vapor deposition (MOCVD), which contains five 1%

* This work has been supported by the Ministry of Science and Technology of China under International Collaborative Research (No.2010DFA61370), the National High-Tech R&D Program of China (No.2013AA014401), and the Natural Science Foundation of Zhejiang Province (No.Z1110276).

** E-mail:kaleemmuk@yahoo.co.uk

compressively strained $\text{In}_{0.8}\text{Ga}_{0.2}\text{As}_{0.8}\text{P}_{0.2}$ QWs with unstrained 1.25Q InGaAsP barriers. The layers of the surface are a 0.5 μm Zn-doped (10^{18} cm^{-3}) InP sacrificial layer, 0.2 μm Zn-doped (10^{19} cm^{-3}) $\text{In}_{0.53}\text{Ga}_{0.47}\text{As}$ cap, 1.5 μm Zn-doped (10^{18} cm^{-3}) InP cladding, 0.004 μm Zn-doped ($4 \times 10^{17} \text{ cm}^{-3}$) 1.3Q InGaAsP etch-stop layer, 0.15 μm Zn-doped ($4 \times 10^{17} \text{ cm}^{-3}$) InP cladding, five repeats of 10 nm undoped InGaAsP barrier ($\lambda_g=1.25 \mu\text{m}$) and 5.5 nm undoped $\text{In}_{0.8}\text{Ga}_{0.2}\text{As}_{0.8}\text{P}_{0.2}$ QW, which are sandwiched by two 0.06 μm InGaAsP step-graded index separate confinement layers with the bandgap wavelength λ_g varying from 1.05 μm to 1.25 μm , and 1.5 μm Si-doped ($2 \times 10^{18} \text{ cm}^{-3}$) InP buffer on Si-doped ($4 \times 10^{18} \text{ cm}^{-3}$) InP substrate. A schematic diagram of the sample is shown in Fig.1.

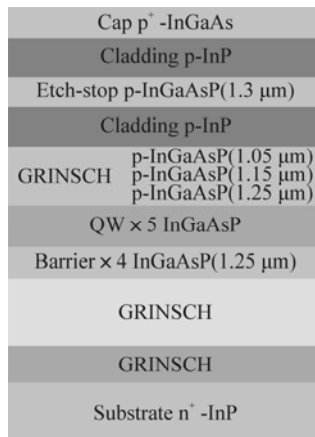


Fig.1 Schematic diagram of the MQW sample used to investigate the UV-QWI technique

To obtain large bandgap blue shift of the InGaAsP/InP laser structure, the sample was irradiated by a KrF excimer laser ($\lambda=248 \text{ nm}$) with pulse duration of 23 ns and high energy of 50 mJ/cm^2 . The sample was irradiated at room temperature and under normal incidence to the surface. The pulse repetition rate was 10 Hz. Without using a mask, spots with almost rectangular shape were created on the sample surface with non-homogenized laser beam. The x - y - z positioning of the sample was controlled by a computer. Since the irradiation window of the setup was only about $600 \mu\text{m} \times 500 \mu\text{m}$ with lower intensity at the edges, the QWI region was obtained by using a step-and-repeat process, with step sizes of 300 μm and 250 μm in the x and y directions, which are smaller than the window sizes to improve the uniformity. After UV-laser treatment, the samples were annealed in a nitrogen atmosphere using an RTA furnace operating at 750 $^\circ\text{C}$ for 120 s. Samples were placed between two Si wafers to prevent desorption of the group V elements during the RTA processing. The possible damage generated during the UV-laser irradiation process is investigated before and after RTA treatment.

Using room temperature PL measurements, the bandgap shifts induced by the UV-laser procedure were meas-

ured. The PL mapper using a Nd:YAG laser ($\lambda=1064 \text{ nm}$) was used as an excitation source along with a photodetector array built in a spectrum analyzer. The altered QW sample was placed on a computer-controlled x - y stage which moved in step of 18 μm . A two dimensional map for the peak wavelength and intensity was measured with the computer software by collecting data as a function of the x - y position. We first measured the wavelength at the peak position of the UV-laser beam profile, and then observed the corresponding intensity of the same point. The PL spectral peak corresponds to the QW electron-hole recombination peak, which is obtained at 1554 nm for the as-grown material.

Fig.2 shows the PL spectra of UV-laser QWI region and the RTA-only region. The PL peak shifts from 1525 nm in the RTA-only region to 1423 nm in the QWI region, with blue shift over 130 nm. The peak intensity is increased by 51%. The FWHM of the UV-laser QWI curve is measured to be 86 nm while that of as-grown material is about 91 nm.

The narrowing of the PL linewidth indicates that the intensity enhancement in this experiment is due to the change of QWs rather than the surface effect as reported in earlier work^[9-11].

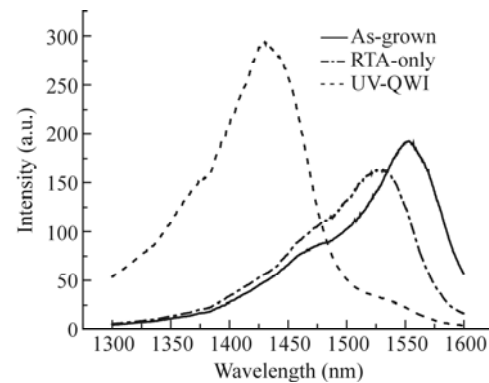


Fig.2 Comparison of PL spectra for InGaAsP/InP samples under different treatments of UV-irradiation plus RTA (QWI) and RTA-only at temperature of 750 $^\circ\text{C}$

The large PL wavelength shift and intensity enhancement at certain UV irradiation conditions can be attributed to the intermixing of round shape QW and the change of strain distribution in the QW that alters the band structure and enhances the Fermi occupation factor.

The above PL spectra prove that laser-induced point defects generated during the UV-laser irradiation and RTA can lead to the fabrication of high-quality QWI material. The process enables relatively large bandgap shift on a single wafer of an InGaAsP/InP laser structure. Such bandgap shifts are attractive for the fabrication of monolithically integrated active-passive devices.

A larger sample ($1.12 \text{ cm} \times 1.25 \text{ cm}$) of InGaAsP/InP laser structure was prepared using UV-QWI procedure to see the versatility of the QWI technique. Fig.3 shows the wavelength map of the sample after UV-laser irradiation

and RTA treatment. It is clear that the UV-QWI region is shifted well over 140 nm while no surface damage is observed.

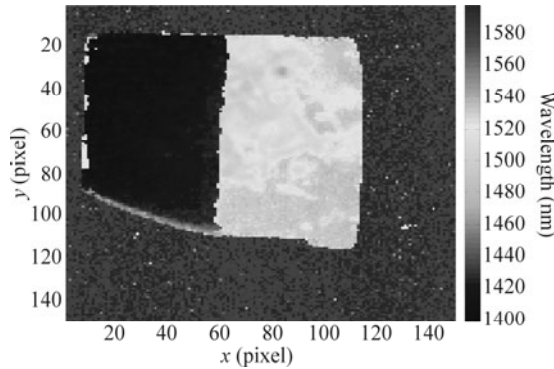


Fig.3 Room temperature PL wavelength map of a KrF laser processed InGaAsP/InP MQW sample after RTA at 750 °C for 120 s

In order to investigate advantages of the UV-laser QWI technique for photonic device fabrication, first we fabricated 3 μm-wide ridge waveguides by standard wet-etching technique, and waveguide loss was measured using the Fabry-Perot (FP) fringe technique. A tunable laser diode (1.46–1.62 μm) was used as the input light source. The light was coupled into the TE mode of the waveguide through a polarization-preserving fiber. The output light was received by a similar fiber, which was coupled into an InGaAs detector built in a spectrum analyzer. When the light scanned the wavelength from 1460 nm to 1620 nm with a step length of 0.01 nm, the output spectra can be obtained.

Fig.4 shows the measured transmission spectra of the as-grown sample and intermixed waveguides cavity. The spectrum of the intermixed waveguides cavity has a blue shift over 100 nm compared with that of as-grown sample. The FP interference fringe is generated due to the multiple reflectances of the two cleaved facets, which is believed to be related to the absorption constant of the waveguide. Therefore, the loss coefficient of waveguide can be derived via these spectra over the measurement wavelength range. At the absorption edge of the as-grown waveguide ($\lambda=1554$ nm), the loss coefficient is measured to be 110 dB/cm, while that of the intermixed waveguide is reduced to only 20 dB/cm. It is a significant reduction of the loss coefficient considering over 100 nm blue shift. By comparing two results, we can find that after intermixing, the loss of the waveguide at the transparent wavelength gets lower. It is possibly due to the partial removal of the defects which exist in the QW region of the as-grown sample. The result also means that the UV excimer induced QWI process does not induce any extra loss to the QW sample.

Secondly, FP laser diodes were fabricated on a similar piece of InGaAsP/InP wafer with one half of the piece undergoing the UV-QWI process and the other half un-

dergoing RTA-only process for comparison. The QWI region was prepared with the same parameters of UV-laser and RTA as before. The length of the fabricated laser diode is 500 μm, and the width is 3 μm.

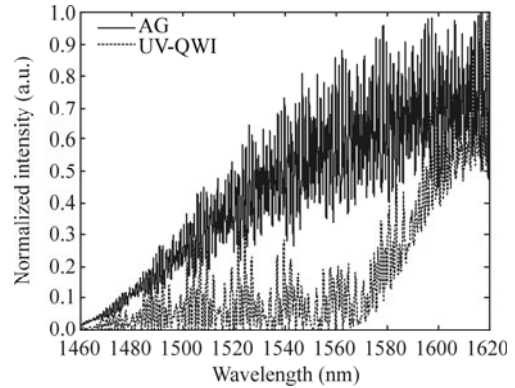


Fig.4 Measured transmitted spectra of intermixed (UV-QWI) and as-grown QW waveguides

Fig.5 shows the voltage versus the injected current ($V-I$) of the UV-QWI based laser and RTA-only laser. Both the curves seem to be normal $I-V$ laser curves. The turn-on voltage of the UV-QWI laser is measured to be 0.82 V while that of the RTA-only laser is about 0.75 V. The large turn-on voltage of the QWI laser is consistent with its larger bandgap as compared with RTA-only laser. The bandgap energy ratio of UV-QWI laser and the RTA-only laser is 1.09 which is the same as the open voltage ratio of the two lasers.

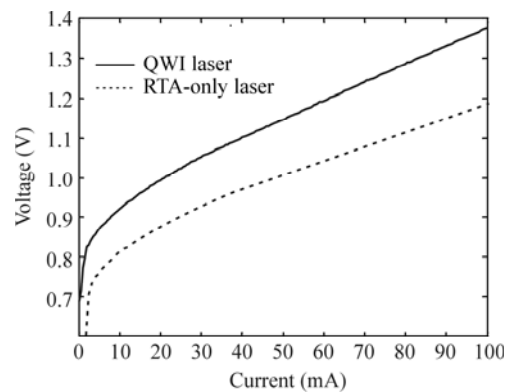


Fig.5 $V-I$ characteristics of UV-QWI laser and RTA-only FP-laser

Fig.6 shows the light power versus the injected current ($L-I$) characteristics of the FP lasers from the UV-QWI region and from the RTA-only region. The UV-QWI processed laser has the threshold current of 29 mA which is lower than that of the RTA-only laser of 36 mA. It shows that after UV-QWI treatment, the loss of the laser cavity decreases, which is consistent with the result of the PL intensity.

Fig.7(a) shows the PL spectra of the UV-QWI laser and RTA-only laser. It is clear that PL of the UV-QWI laser is shifted well over 140 nm, and the corresponding

FWHM is also narrow. Fig.7(b) shows the electroluminescence (EL) spectra of both lasers measured at 15 mA. The EL spectrum of the UV-QWI laser is narrower than that of RTA-only laser, which further confirms the effectiveness of the technique. Fig.7(c) shows the emission spectra of the UV-QWI laser and the RTA-only laser. The UV-QWI laser emission spectrum is obtained at current of 32 mA, while the current of 45 mA is used to obtain the RTA-only laser emission spectrum. The emission peak of the UV-QWI laser is blue shifted from 1542 nm to 1407 nm, while the profile of the laser spectrum remains the same essentially. It further confirms that under appropriate conditions this QWI technique does not affect the lasing property of the material while achieving a large blue shift.

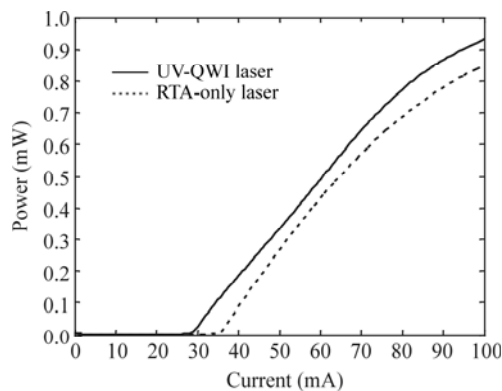


Fig.6 L-I characteristics of the UV-QWI laser and the RTA-only laser

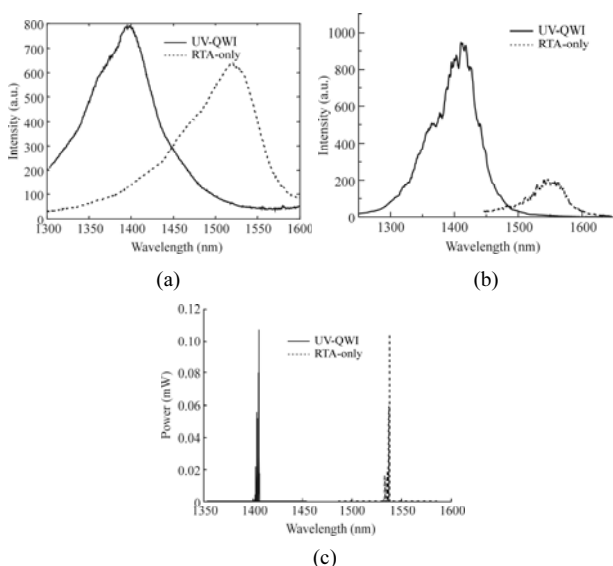


Fig.7 (a) PL spectra, (b) EL spectra and (c) emission spectra of the UV-QWI laser and RTA-only laser

We demonstrate the UV-laser QWI technique to investigate bandgap engineering of compressively strained InGaAsP/InP QW laser microstructures. By using simple excimer laser irradiation followed by RTA, a blue shift as large as 145 nm is achieved in the investigated material. One of the attractive features of this approach is that the PL intensity of the laser processed material can be enhanced, and there is a negligible presence of defects responsible for the deterioration of the photonic properties of the material. Low loss ridge waveguides and low threshold current FP-laser diodes are also demonstrated. We also compare the emission spectra of QWI laser and RTA-only laser. The experimental results demonstrate the potential of the UV-laser QWI technique for the fabrication of integrated multi-bandgap photonic devices.

Acknowledgement

We thank Prof. J. J. Dubowski for his valuable and fruitful discussions.

References

- [1] J. H. Marsh, O. P. Kowalski, S. D. MacDougall, B. C. Qiu, A. McKee, C. J. Hamilton, R. M. De La Rue and A. C. Bryce, *J. Vac. Sci. Technol. A*, **16**, 810 (1998).
- [2] J. H. Marsh, *Semicond. Sci. Technol.*, **8**, 1136 (1993).
- [3] S. Charbonneau, E. S. Koteles, P. J. Poole, J.-J. He, G. C. Aers, J. E. Haysom, M. Buchanan, Y. Feng, A. Delage, F. Yang, M. Davies, R. D. Goldberg, P. G. Piva and I. V. Mitchell, *IEEE Journal of Selected Topics in Quantum Electron.*, **4**, 772 (1998).
- [4] J.-J. He, Y. Feng, E. S. Koteles, J. P. Poole, M. Davis, M. Dion, R. Goldberg, I. Mitchell and S. Charbonneau, *Electronics Letters*, **31**, 2094 (1995).
- [5] X. Zhang and J.-J. He, *Optical Loss of Bandgap Shifted InGaAsP/InP Waveguide Using Argon Plasma-Enhanced Quantum Well Intermixing*, *Advances in Optoelectronics and Micro/Nano-Optics*, 2010.
- [6] O. P. Kowalski, C. J. Hamilton, S. D. MacDougall, J. H. Marsh, A. C. Bryce, R. M. De La Rue, B. Vogeles and C. R. Stanley, *Appl. Phys. Lett.*, **72**, 581 (1998).
- [7] M. Kaleem, Xin Zhang and Jian-Jun He, *Bandgap Engineering of InGaAsP/InP Laser Structure by Argon Plasma Induced Point Defects*, *Asia Communications and Photonics Conference*, 2012.
- [8] J. Genest, R. Beal, V. Aimez and J. J. Dubowski, *Appl. Phys. Lett.*, **93**, 071106 (2008).
- [9] J. J. Dubowski, P.J. Poole, G.I. Sproule, G. Marshall, S. Moisa, C. Lacelle and M. Buchanan, *Appl. Phys. A*, **69**, S299 (1999).
- [10] N. Liu, K. Moumanis, S. Blais and J. J. Dubowski, *Proc. SPIE*, **8245**, 82450E1 (2012).
- [11] N. Liu and J. J. Dubowski, *Appl. Surf. Sci.*, **270**, 16 (2013).